



# Has nitrogen availability decreased over much of the land surface in the past century? A model-based analysis

Peter M. Vitousek · Xiaoyu Cen ·  
Peter M. Groffman

Received: 16 October 2023 / Accepted: 18 April 2024  
© The Author(s) 2024

**Abstract** A recent publication (Mason et al. in *Science* 376:261, 2022a) suggested that nitrogen (N) availability has declined as a consequence of multiple ongoing components of anthropogenic global change. This suggestion is controversial, because human alteration of the global N cycle is substantial and has driven much-increased fixation of N globally. We used a simple model that has been validated across a

climate gradient in Hawai‘i to test the possibility of a widespread decline in N availability, the evidence supporting it, and the possible mechanisms underlying it. This analysis showed that a decrease in  $\delta^{15}\text{N}$  is not sufficient evidence for a decline in N availability, because  $\delta^{15}\text{N}$  in ecosystems reflects both the isotope ratios in inputs of N to the ecosystem AND fractionation of N isotopes as N cycles, with enrichment of the residual N in the ecosystem caused by greater losses of N by the fractionating pathways that are more important in N-rich sites. However, there is other evidence for declining N availability that is independent of  $^{15}\text{N}$  and that suggests a widespread decline in N availability. We evaluated whether and how components of anthropogenic global change could cause declining N availability. Earlier work had demonstrated that both increases in the variability of precipitation due to climate change and ecosystem-level disturbance could drive uncontrollable losses of N that reduce N availability and could cause persistent N limitation at equilibrium. Here we modelled climate-change-driven increases in temperature and increasing atmospheric concentrations of  $\text{CO}_2$ . We show that increasing atmospheric  $\text{CO}_2$  concentrations can drive non-equilibrium decreases in N availability and cause the development of N limitation, while the effects of increased temperature appear to be relatively small and short-lived. These environmental changes may cause reductions in N availability over the vast areas of Earth that are not affected by high

---

Responsible Editor :Sharon A. Billing

---

**Supplementary Information** The online version contains supplementary material available at <https://doi.org/10.1007/s10533-024-01146-y>.

---

P. M. Vitousek (✉)  
Department of Earth System Science, Stanford University,  
Stanford, CA 94305, USA  
e-mail: vitousek@stanford.edu

X. Cen  
Institute of Geographic Sciences and Natural Resources  
Research, Beijing 100101, China

X. Cen  
College of Resources and Environment, University  
of Chinese Academy of Sciences, Beijing 100049, China

P. M. Groffman  
City University of New York, Advanced Science Research  
Center at the Graduate Center, New York, NY 10031, USA

P. M. Groffman  
Cary Institute of Ecosystem Studies, Millbrook,  
NY 12545, USA

rates of atmospheric deposition and/or N enrichment associated with urban and agricultural land use.

**Keywords** Carbon dioxide · Climate change · Disturbance · Nitrogen · Nitrogen-15 · Phosphorus

## Introduction

Nitrogen (N) and phosphorus (P) as well as carbon (C) are among the element cycles that have been most consequentially altered by human activity in the Anthropocene. For both N and P, the most important cause of alteration is the production and use of industrial fertilizer in conventional agriculture. In both cases, fertilizer production globally exceeds the background fluxes of N (through biological N fixation [BNF] in natural ecosystems and lightning) and P (through weathering of rocks and minerals in natural ecosystems) several-fold (Bennett et al. 2001, Galloway et al. 2008; Falkowski et al. 2008; Vitousek et al. 2013). In addition, there are other pathways for mobilization of N, notably BNF in agriculture (Herridge et al. 2008) and fossil fuel (especially coal) combustion (Fowler et al. 2013; Liu et al. 2013), and additional industrial uses for both elements that draw upon anthropogenically fixed N and mined P (Gu et al. 2015; Wang et al. 2015).

Differences in the dynamics of N and P are important when fertilizer is applied to agricultural fields. Fertilizer P is largely immobile, while N can move in soluble forms by a variety of pathways to downstream and downwind ecosystems. This movement is especially marked where fertilizer applications are excessive and/or not synchronized with crop uptake, which is difficult to accomplish for annual crops for which there is a time of year (the non-growing season) when no crop is taking up nutrients. Consequently, the largest losses of P from agricultural systems are in harvest and in the erosion of agricultural soils, while losses of N are larger and occur by multiple pathways to harvest and erosion (as for P), downstream and to groundwater by leaching of mobile nitrate, and downwind following volatilization by a variety of processes.

A recent publication by Mason et al. (2022a) suggested that N availability has decreased in the past century outside of the regions where the N cycle is altered most substantially. They suggest

that this decrease is a consequence of other global change factors, especially increasing atmospheric CO<sub>2</sub> concentrations, which cause decreasing concentrations of all nutrients (including N and P) in plant tissues. This suggestion is controversial. A response by Olf et al. (2022) suggested that air quality regulations could have decreased N availability in recent decades, and that some of the evidence summarized by Mason et al. (2022a) for decreasing N availability (particularly the declining  $\delta^{15}\text{N}$  in tree rings, lake sediments, and plant tissues) could reflect a changed mixture of <sup>15</sup>N sources reaching downwind ecosystems. Mason et al. (2022b) responded that the decline in N availability began well before air quality regulations took effect, and that any change in the mixture of <sup>15</sup>N sources would have to be unrealistically large to have the effects that Olf et al. (2022) suggested.

A decline in N availability would be particularly important if it induced or exacerbated N limitation to primary productivity, which would likely be the case because once N supply equilibrated with N demand by plants, any increase in plant production (and so plant demand for N) or any loss of N or any decrease in the rate of N cycling would both decrease N availability and induce N limitation (Vitousek 2004), assuming that the change was rapid enough that it was not offset by continued N inputs. A recent model-based analysis by Vitousek et al. (2022), following earlier publications by Vitousek and Field (1999) and Menge et al. (2008) demonstrated that at equilibrium, N limitation to primary production that is more than marginal and/or ephemeral requires both losses of N that cannot be prevented by N-limited biota and constraints that keep BNF from responding to N deficiency. The Vitousek et al. (2022) publication focused on uncontrollable losses of N, and demonstrated that losses of dissolved organic nitrogen (DON) (which are not a component of anthropogenic global change), asynchronies in the supply and demand for N caused by variation in precipitation (which is increasing and likely will continue to increase as the climate changes (Kharin et al. 2007; Pendergrass et al. 2017)), and widespread changes in land use like harvest and fire all represent losses of N that cannot be controlled by N-limited biota.

In this paper, we apply simple models of N cycling that have been validated across a climate gradient on the Island of Hawai'i (Vitousek et al. 2021) to reveal general trends of N availability change and to evaluate whether

components of anthropogenic global change can cause widespread decreases in N availability. We use simple models to reveal a general trend of N availability change, because unlike changes in carbon cycle (which are often easily-observed structural changes such as biomass or C pool changes), changes in the N cycle are usually functional (such as changes in N concentrations in organisms, and the consequent changes in N fluxes) which are more challenging to observe and to analyze. Modeling approaches are often used when observational data do not suffice to reveal spatial/temporal patterns. Complex models (such as full ecosystem models) that comprehensively simulate ecosystem processes and interactions are powerful tools for quantitative analysis, although under-represented N cycling processes in many models and also insufficient observational data for model parameter calibrations reduce the applicability of such complex models for simulating N availability change over large spatial/temporal scales (Stocker et al. 2016). In this situation, simplified models may be particularly useful for exploring a general trend on large scales, considering that such models are designed for a handful of objects/processes with lower demands for input data.

## Methods

We used simple models developed by Vitousek et al. (2021, 2022) to evaluate the effects of increasing temperature, increasing atmospheric concentrations of CO<sub>2</sub>, temporal variability in precipitation, and ecosystem-level disturbance on N availability and on N limitation to NPP (net primary productivity), and changes in the atmospheric deposition of <sup>15</sup>N on δ<sup>15</sup>N pools within ecosystems. This class of models was described in detail in Vitousek et al. (2021), and modifications were described in Vitousek et al. (2022); here (since our focus is on changes in N availability), we reproduce and update the description of how the N cycle (including <sup>15</sup>N) and NPP are simulated.

This class of models represents relevant portions of the cycles of N and P, but make no effort to be complete ecosystem models. We therefore regard them as “toy” models, which are defined as simplified sets of objects and equations that can be used to understand mechanisms. We find such models particularly useful for testing understanding of the implications of biogeochemical processes.

Although the models we use here are relatively complex, we call them toy models because their purpose is to explore general principles rather than to capture the quantitative details of a particular system. In the sense of Rastetter (2017), these are models designed to further understanding rather than models designed to yield specific predictions.

The structure of the portion of the toy model that is focused on N is as follows. N enters ecosystems through atmospheric deposition (which we treat as a linear function of precipitation, as for Ca and P) and through biological N fixation. N also can be added as fertilizer, to test for N limitation to net primary production (NPP). N is lost through ammonia volatilization, nitrate loss (which could be due to nitrate leaching or denitrification), transformation-dependent trace gas losses (defined below), and dissolved organic N (DON) leaching. For each input or loss pathway, we calculate inputs/outputs of both all N and of <sup>15</sup>N separately, and we assume a level of isotopic abundance (for losses of N, isotopic fractionation) associated with each pathway of input/loss. For inputs, we assume no isotopic discrimination associated with fertilizer or biological N fixation (so <sup>15</sup>N enters ecosystems by these pathways at the average value of 0.003663 of total N, for a δ<sup>15</sup>N of 0‰). For atmospheric deposition, we assume deposited N is 5 per mil depleted (-5‰), based on observations of N isotopes in non-N-fixing lichens without access to soil N in Hawai‘i (Vitousek et al. 1989). For the within-ecosystem cycling of N, we calculate N mineralization as:

$$N_{\min} = \text{SoilorgN} - \frac{\text{SoilorgC}}{\text{CN}_{\text{crit}}}$$

(with a critical C:N ratio (CN<sub>crit</sub>) of 20), setting N mineralization for that time step to 0 when the calculation yields negative N mineralization, and we calculate nitrification as a variable fraction (varying with climate, as described below) of the ammonium-N pool remaining in the soil after N mineralization and after plant N uptake by the non-N-fixer.

Pathways of N loss will be discussed individually. Ammonia volatilization is pH-dependent; pH is not simulated directly in the model, so we use the mineral Ca pool in the soil as an index of soil pH. Our reasoning is that weathering is the main buffer of acidity in the soil here (Chadwick and Chorover 2001), and high

concentrations of mineral Ca in the soil reflect ongoing weathering and so lower acidity than in older or more fully leached areas. Ammonia volatilization is calculated as 10% of the ammonium pool in the surface soil layer (after plant uptake and nitrification) times the index of soil pH (so that when Ca and so pH is low, ammonia volatilization approaches 0); we assume that the heavy isotope of N ( $^{15}\text{N}$ ) is discriminated against by 1.5% (so a fractionation of -15 ‰ for ammonia volatilization (Ti et al. 2021; Peng et al. 2022), making the remaining N in the system  $^{15}\text{N}$ -enriched.

Nitrate loss could occur by either leaching of nitrate through the soil or through denitrification. We believe that on this Hawai'i climate gradient, most of the nitrate loss occurs via leaching. Our reasoning is that (1) nitrate pools in the soil are very low in the high-rainfall sites on the climate gradient (von Sperber et al. 2017), an observation consistent with either leaching or denitrification; and (2)  $\delta^{15}\text{N}$  of the N in the small amount of nitrate in high-rainfall sites is strongly  $^{15}\text{N}$ -depleted (von Sperber et al. 2017) a result consistent with nitrification of only a fraction of the soil ammonium pool and subsequent leaching losses, but inconsistent with denitrification of a substantial fraction of the nitrate, because denitrification would leave the residual nitrate-N  $^{15}\text{N}$ -enriched (Houlton et al. 2006). Accordingly, we calculate rates of nitrification that decline from low-rainfall into high-rainfall sites, and we estimate nitrate losses as the fraction of soil water at WHC that leaches each month (up to leaching=WHC, above that point we assume no further increase in leaching) times the nitrate pool in the soil. We assume that the heavy isotope of N ( $^{15}\text{N}$ ) is discriminated against by 1.0% (so a fractionation of -10 ‰ for nitrification and subsequent nitrate losses), thereby making the remaining N in the system  $^{15}\text{N}$ -enriched. This assumption is consistent with von Sperber et al.'s (2017) measurements of  $^{15}\text{N}$  in nitrate; this assumed fractionation is less than reports of kinetic isotope fractionation during nitrification (Mariotti et al. 1981), but the co-occurrence of nitrification (by multiple pathways) and denitrification in real ecosystems (Granger and Wankel 2016), together with the extent to which reactions go to completion, makes applying kinetic isotope fractionations to real ecosystems problematic. Episodic denitrification could be more important than it was during von Sperber et al.'s sampling, and so

greater than we assume here; if so, it is possible that the fractionation associated with nitrate loss could be greater. While incomplete nitrification leads to an  $^{15}\text{N}$  depleted nitrate pool (as von Sperber et al. (2017) observed), and denitrification would then fractionate that pool a little less than did nitrification (Mariotti et al. 1981), with a lower overall fractionation for the whole process from ammonium to  $\text{N}_2$  than for nitrate leaching. However, more rapid and complete nitrification (at the limit, of the whole ammonium pool) would not lead to fractionation of nitrate relative to ammonium, and denitrification could then cause a greater overall isotopic fractionation associated with nitrate loss. In any case, fractionating losses of N can have cumulative effects that enrich the residual N remaining in ecosystems.

Transformation-dependent losses of N-containing trace gases represent our effort to represent losses of N that occur during nitrification. We estimate this flux at 1% of nitrification (Firestone and Davidson 1989). We consider those losses to differ in kind from ammonia volatilization and nitrate leaching or denitrification, both of which occur from accumulated pools of biologically-available N that remains in the soil after organisms have acquired the N that they can. In this sense, we regard both ammonia volatilization and nitrate leaching and/or denitrification to be losses that are controllable by organisms, in that those organisms (if their activity would otherwise be constrained by a shortage of N) could prevent those losses; we regard transformation-dependent losses to be uncontrollable, in that they will occur if there is nitrification even if N is in short supply in the ecosystem. In practice, simulated transformation-dependent N trace gas losses represent a small fraction of N losses from unfertilized sites across the gradient we studied.

Losses of DON also are assumed to represent uncontrollable losses of N (Hedin et al. 1995), in that the organic N compounds that leach through soils are large-molecular-weight recalcitrant compounds that are not readily taken up by organisms (Perakis and Hedin 2001, 2002). We calculate losses of DON from all the sites on the climate gradient as representing a maximum of 0.1% of soil organic N per month times the fraction of soil water at WHC that is leached each month (again with no further increase in DON loss if leaching is greater than WHC during that month).

We simulate plant productivity following the procedure in Vitousek and Field (1999), adjusted to a monthly rather than an annual time step by dividing their maximum potential productivity and the N and P supply necessary to support that productivity by 12. We simulate the growth both of a non-N-fixing plant and of a symbiotic N-fixing plant; the two differ in that the N-fixer has an N- and P-rich stoichiometry relative to the non-fixer (McKey 1994; Menge 2011) (C:N:P for the non-fixer is 500:10:1, while that for the N-fixer is 333.3:10:1), and in that the N-fixer is an obligate fixer (it derives all of its N from fixation) (Menge et al. 2009). Both the fixer and non-fixer are assumed to be perennial plants whose tissues (and N and P contents) turn over at a rate of 1%/month. For the non-fixer, potential productivity per month is assumed to represent an (implicitly light-limited) maximum, reduced in practice by the supply of N or P (whichever is in shorter supply relative to plant demand) and by a climate scalar calculated based on multiplicative constraint by soil water content and by temperature. That constraint is calculated as:

$$\text{prodscalar1}(y) = \left( \frac{\text{soilwater1}(y)}{3} \right) * \left( \frac{\text{Temp}(v)}{25} \right)$$

where  $\text{prodscalar1}(y)$  is the climatic constraint to potential productivity,  $y$  is the month of simulation,  $\text{soilwater1}(y)$  is the water content of the soil to 30 cm depth (in cm of water/10—additionally,  $\text{prodscalar1}(y)$  is set to 0 when  $\text{soilwater1}(y) < 0.5$ , representing a permanent wilting point), 3 represents the WHC of the soil/10 (30 cm of water), and  $\text{Temp}(v)$  is the mean temperature (in °C) at that point on the climate gradient.

We calculate a cost of N acquisition for the non-fixer as in Vitousek and Field (1999); that cost is assumed to be low when N is abundant but the cost increases as the N pool is depleted (Vitousek et al. 2022).

For the N-fixer, we assume a fixed cost of N fixation (30% of plant NPP goes to support N fixation). The non-fixer makes use of all of the potential productivity up to the point where its cost for acquiring N exceeds that of the N-fixer. Beyond that point, the N fixer (alone) grows and derives all of its N from fixation. The growth of the N fixer is independent of soil N supply; however, the N-fixer can be constrained by the remaining productive

capacity of the site (implicit light limitation) after use of a portion of that capacity by the non-fixer, by climate, and/or by P supply (Vitousek and Field 1999). In addition, the growth of both plants is constrained when their biomass is low (they cannot jump all the way to their potential productivity in one time-step), and the growth of the N-fixer is further constrained by a function representing shading by the non-fixer (which reduces the energy available to support N fixation). Both of these constraints are calculated as in Vitousek and Field (1999), adjusted to the monthly time step of the present toy model.

For both plants, we calculate several possible rates of production based on potential productivity (implicitly light-limited) and the productivity that can be supported by biologically-available P and N—for non-fixers (the productivity of N-fixer can be constrained by P but not N). All of these estimates of productivity can be further constrained by soil water, temperature, a low initial biomass, and for the N fixer by shading by the non-fixer. The minimum of these estimates of productivity is then selected and applied to calculate uptake of N and P based on the fixed C:N:P stoichiometry of each plant. Inputs of N through BNF are calculated as the NPP of the N-fixer times its (fixed) N:C ratio; biologically fixed N becomes available in the system as a whole when litter from the N-fixer enters the soil organic C and N pools, and is mineralized as described above. Also, atmospheric inputs of N are assumed to be biologically available.

We modified the program *tnewprodnofixer* (Vitousek et al. 2022) to evaluate the effects of increased temperature and elevated atmospheric concentrations of CO<sub>2</sub> on N biogeochemistry. This program (in MATLAB version 2018a) is available as on-line supplementary material associated with this article. All runs of the model shown here were carried out with a simulated mean monthly precipitation of 20 cm/month, where there is leaching of nitrate under average conditions and which is also the point on the climate gradient where N limitation was maximized (Vitousek et al. 2022). We also carried out a complete set of model runs at 10 cm/mo precipitation. We modeled the effects of increasing CO<sub>2</sub> by increasing the potential productivity of plants and changing the stoichiometry of their tissues (making them more C-rich and nutrient-poor) without changing the critical C:N and C:P ratios for nutrient release during decomposition (these changes had the effects of



increasing potential productivity and slowing the rate of N cycling). Plants that respond to elevated CO<sub>2</sub> with increased growth (including most C3 plants) typically have lower tissue concentrations of nutrients as well (Penuelas et al. 2020). The observed increase in CO<sub>2</sub> concentrations has followed an exponential path, but we modeled it as a linear increase. We do not yet know whether, where, and how increasing atmospheric concentrations of CO<sub>2</sub> will end; we modeled them as beginning to increase after 45,000 time steps (months) (or 3750 years) of model runs (when biomass and N cycling had equilibrated), continuing to increase for 125 years, and ceasing their increase when potential productivity and C/nutrient ratios in plant tissue had increased a pre-selected amount—and then remaining in that state (with atmospheric CO<sub>2</sub> concentrations still elevated) for the remainder of the run, which ended after 5000 years. Temperature increases were modeled similarly, beginning to increase after 3750 years of simulation, increasing linearly for 125 years, then remaining elevated to the end of the model run. Other scenarios could be simulated equally well. BNF was turned off in these

simulations, because where BNF is unconstrained, it responds rapidly to N limitation and reverses it, even though growth of the N-fixer is strongly constrained in the model as described above.

## Results and discussion

Because  $\delta^{15}\text{N}$  integrates multiple processes which can fractionate it in different directions, it is a useful integrator of the N cycle (Robinson 2001) but it not easy to model correctly—however, the agreement in pattern between results of the toy model and field observations (von Sperber et al. 2017) is striking (Fig. 1). Figure 1 shows a comparison between observed  $^{15}\text{N}$  in soils and modeled whole-system  $^{15}\text{N}$ ; soils accounted for 65–93% of modeled total N in the system (depending on rainfall/water balance). Observations and simulation results differ most in intermediate-rainfall and wetter sites on the gradient, where observations yield soil  $\delta^{15}\text{N}$  that is a few ‰ enriched in  $^{15}\text{N}$ , while simulations yield little enrichment (or slight depletion) in  $\delta^{15}\text{N}$ . The difference

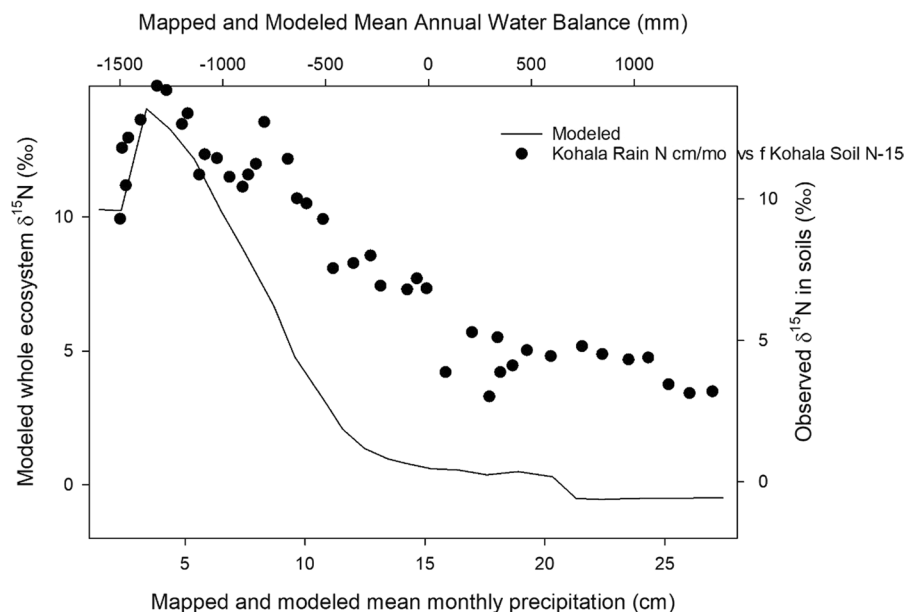


**Fig. 1** Observed  $\delta^{15}\text{N}$  in soils (points) and modeled  $\delta^{15}\text{N}$  in ecosystem N (line) on the Hawai‘i climate gradient. Observations from von Sperber et al. (2017). This figure shows a comparison between observed  $^{15}\text{N}$  in soils and modeled whole-system  $^{15}\text{N}$ ; soils accounted for 65–93% of modeled total N in the system (depending on rainfall/water balance). In this figure,

we label the lower X-axis as Mapped and Modeled Mean Monthly Precipitation (in cm/month). The upper X-axis shows annual water balance (precipitation (ppt) minus Potential EvapoTranspiration (PET)) in mm/yr. Mapped precipitation and water balance results from Giambelluca et al. (2013). This figure is reproduced from Vitousek et al. (2021)

could be due to an underestimate of denitrification (and its associated fractionation of the lost N), or to partial preservation of  $^{15}\text{N}$ -enriched organic matter on short-range ordered clay minerals in wetter sites (Kramer et al. 2012). Both observations and simulations then show an increase in enrichment in drier sites to a peak near +14‰, then a decline in enrichment below ~3.5 cm/mo precipitation (–1400 mm/year water balance). This decline in enrichment from moderately dry sites into the driest sites also is observed for  $^{15}\text{N}$  in nitrate (von Sperber et al. 2017) and for  $^{15}\text{N}$  in the tissues of non-N-fixing plants (Burnett et al. 2022) on this gradient. The sensitivity of  $\delta^{15}\text{N}$  to differing assumptions concerning parameter values is relatively small (Vitousek et al. 2022);  $\delta^{15}\text{N}$  follows the same pattern across the gradient for a wide range of assumptions about the values of driving variables (Vitousek et al. 2022)—with the exceptions that assumptions about  $\delta^{15}\text{N}$  in inputs and losses

of N can have substantial effects on the results, as can the empirical observation that there are few and relatively inactive N fixers in the driest sites.

Results of this analysis for the effects of changes in the temporal variability of precipitation and for disturbance (including harvesting, fire, and windthrow) on N limitation to plant biomass were published earlier (Vitousek et al. 2022). Both of these changes cause losses of N that cannot be controlled by N-limited organisms and so can induce N limitation if there are constraints to BNF. Here we evaluate NPP directly, and demonstrate that N limitation is associated with (caused by) a decrease in N availability for both temporal variation in precipitation and for disturbance (Figs. 2, 3). (N limitation in the model is defined by the difference in productivity with and without added N.) In tropical regions, disturbance has the effect of converting primary forests (which are often limited by P) to N-limited secondary forests (Davidson et al.

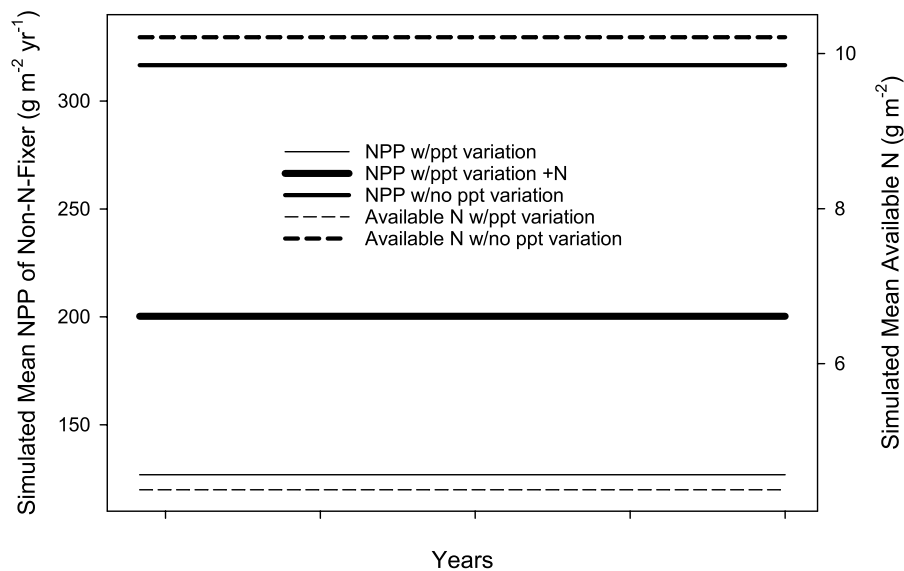


**Fig. 2** Simulated effects of increasing temporal variation in precipitation on the NPP of a non-N-fixing plant and on N availability (calculated as the sum of N mineralization, atmospheric deposition of N, carryover of inorganic N from the previous time step [if any], and N fertilization [if any]) and on N availability, calculated at a precipitation level of 20 cm/month using the program *tnewprodnofixer* with BNF turned off. Because NPP and available N are highly variable at this level of temporal variation in precipitation, mean values are plotted here. The coefficient of variation (CV) at 20 cm rain/month is 0.79; we used an increased variation with a CV of 1.18 here (equivalent to that observed at 10 cm/month on the gradient). NPP is plotted with solid lines here and avail-

able N with dashed lines; thin lines are used for NPP and N availability with increased temporal variation in precipitation, intermediate-thickness lines for NPP and N availability with no temporal variation in precipitation, and a thick line for NPP with N fertilization and increased temporal variation in precipitation. Compare NPP with and without N fertilization for the effect of temporal variation in precipitation on N limitation; and compare N availability with and without temporal variation in precipitation for the effect of that variation on N availability. There is no N limitation without temporal variation in precipitation, so the effects of N fertilization are not plotted for that case, and N availability is very high with N fertilization, so that is not plotted either

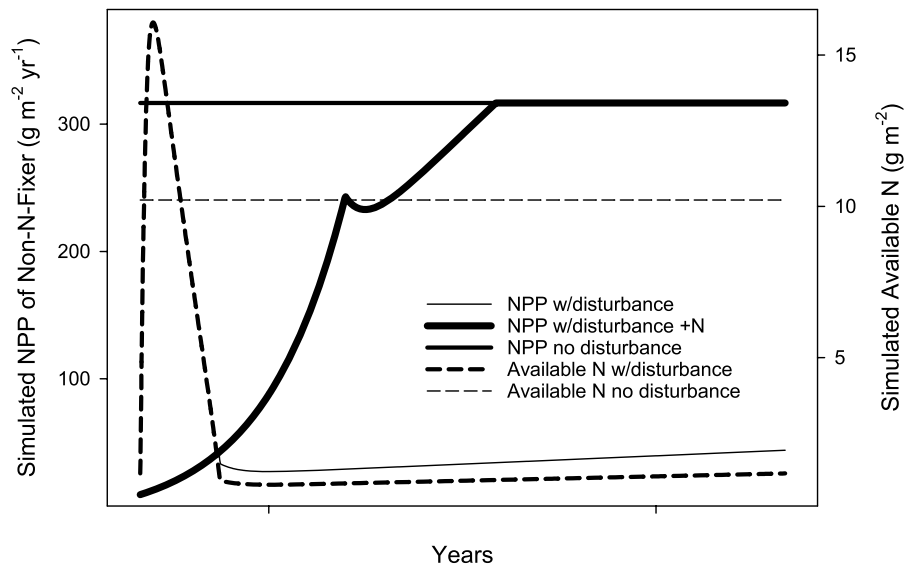


**Fig. 3** Simulated effects of disturbance (here harvest, simulated by removing all the N and P in plant biomass every 83.33 years after an initial equilibration period of 3750 years) on the NPP of a non-N-fixing plant and on N availability (calculated as described in the legend for Fig. 2), calculated at a precipitation level of 20 cm/month using the program *tcnewprodnofixcr* with BNF turned off. The 11th occurrence of disturbance is shown here. NPP is plotted with solid lines here and available N with dashed lines; thin lines are used for NPP and N availability with disturbance, intermediate-

thickness lines for NPP and N availability with no disturbance, and a thick line for NPP with N fertilization and disturbance. Compare NPP with and without N fertilization for the effect of disturbance on N limitation; compare N availability with and without disturbance for the effect of disturbance on N availability. There is no N limitation without disturbance, so the effects of N fertilization are not plotted for that case, and N availability is very high with N fertilization, so that is not plotted either

2004). Here we also evaluate the effects of increasing temperature (Fig. 4) and increasing atmospheric concentrations of CO<sub>2</sub> (Fig. 5) on N availability and N limitation, both with and without N added as a direct test of N limitation within the model. The model is useful here because we can evaluate direct effects of increasing atmospheric CO<sub>2</sub> concentrations, increasing temperature, and increasing variability in precipitation separately, although in practice they all occur together.

The results of these analyses are clear; the effects of elevated atmospheric CO<sub>2</sub> concentrations is to reduce N availability, and to induce N limitation to plant growth (Fig. 6). This N limitation is non-equilibrium—it reverses eventually because of the slow accumulation of N from atmospheric deposition—unlike the effects of increased temporal variability in precipitation or increased disturbance, which continue as long as forcing persists. While there is an increase in NPP induced by a 4 °C temperature increase (Fig. 5), it occurs slowly enough that even

the low rate of atmospheric deposition modeled here can prevent a substantial decrease in N availability or the development of N limitation. In contrast, increasing atmospheric CO<sub>2</sub> (Fig. 5) both increases potential productivity and slows the rate of N cycling (the latter change being the more important one), so its effect on N availability and N limitation is relatively large and long-lasting. Given a 1.25-fold increase in potential productivity and C:element ratios in plant tissue, the maximum increase in the extent of N limitation to NPP at current levels of temporal variation in precipitation would be 16%, and the effect would not disappear for almost 300 years (Fig. 6a). There might be positive feedbacks where decreases in soil N availability accelerate changes in C:element ratios as plants increase resorption of N (Groffman et al. 2018). Model runs at 10 cm/mo of precipitation yielded qualitatively similar results. It should be reiterated that both atmospheric CO<sub>2</sub> concentrations and temperature remain elevated here (after increasing for 125 years) for the remainder of the model run. This



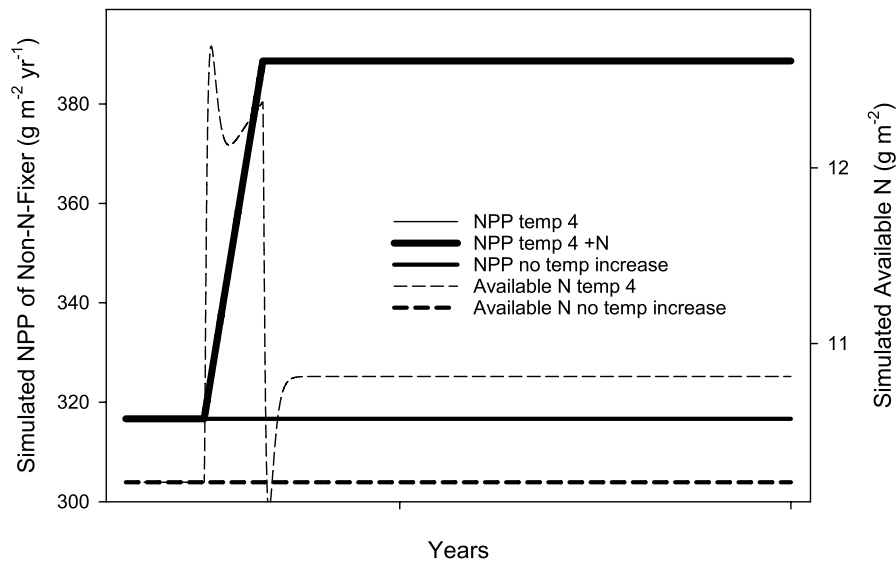


**Fig. 4** Simulated effects of increasing temperature on the NPP of a non-N-fixing plant and on N availability (calculated as described in the legend of Fig. 2), calculated at a precipitation level of 20 cm/month using the program *tcnewprodnofixer* with BNF turned off. In this run, temperature began increasing in year 3750 and increased 4 °C over 125 years, and then remained elevated to the end of the run. Fertilization with N also began in year 3750 and continued to the end of the run. NPP is plotted with solid lines here and available N with dashed lines; thin lines are used for NPP and N availability with increasing temperature (the thin solid line here is entirely

underneath the thick solid line), intermediate-thickness lines for NPP and N availability with no temperature increase, and a thick line for NPP with N fertilization and increasing temperature. Compare NPP with and without N fertilization for the effect of temperature increase on N limitation; compare N availability with and without disturbance for the effect of increasing temperature on N availability. There is no N limitation without increasing temperature, so the effects of N fertilization are not plotted for that case, and N availability is very high with N fertilization, so that is not plotted either

simulation shows that the change in plant stoichiometry and increase in potential productivity caused by elevated CO<sub>2</sub> is a plausible cause of declining N availability and increasing N limitation, as suggested by Mason et al. (2022a, b) supporting earlier suggestions by Hungate et al. (2003)

We used the model to evaluate a range of increased temperatures, increased atmospheric CO<sub>2</sub> concentrations, and increased temporal variations in precipitation (Fig. 6a, b). We examined 4 levels each of change in potential productivity and C:element ratios (our proxy for changes in atmospheric concentrations of CO<sub>2</sub>), temperature change, and temporal variability in precipitation. We do not know what the changes in these features of global change have been or will be, but we suspect that changes in CO<sub>2</sub> will have larger effects than changes in temperature in the maritime environment of Hawai‘i where the model was first applied. We do not know that current month-to-month variability in precipitation has a coefficient of

variation of ~0.78 in wetter portions of the gradient, equivalent to the 2nd level tested in the simulation. Figure 6a shows the maximum extent of N limitation resulting from these changes in climate or CO<sub>2</sub>, while Fig. 6b shows how many years it takes for atmospheric deposition to overcome the N limitation caused by the change. There is no line for the effects of increased temporal variation in precipitation in Fig. 6b because it represents an equilibrium change, which will not be overcome by ongoing atmospheric deposition.

We also used a version of the toy model to evaluate changes in δ<sup>15</sup>N because a decline in <sup>15</sup>N was used as evidence for declining N availability by Mason et al. (2022a), and this was an area of disagreement between Mason et al. (2022a,b) and Olff et al. (2022). Publications by Vitousek et al. (2021) and Burnett et al. (2022) evaluated δ<sup>15</sup>N in soils and plants (respectively) across this broad precipitation gradient (285–3240 mm/year) in an unpolluted region on the

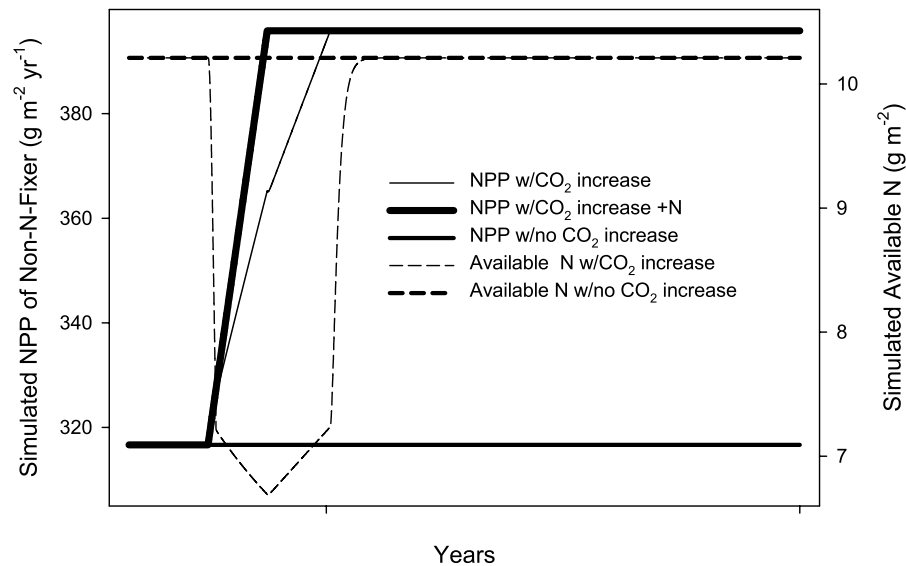


**Fig. 5** Simulated effects of increasing atmospheric  $\text{CO}_2$  on the NPP of a non-N-fixing plant and on N availability (calculated as described in the legend of Fig. 2) and N limitation, calculated at a precipitation level of 20 cm/month using the program *tnewprodnofixcr* with BNF turned off. In this run, atmospheric  $\text{CO}_2$  began increasing in year 3750 and increased to the point that potential productivity and C/N and C/P ratios increased 1.25-fold over 125 years, and then remained elevated to the end of the run. Fertilization with N also began in year 3750 and continued to the end of the run. NPP is plotted with solid lines here and available N with dashed lines; thin lines

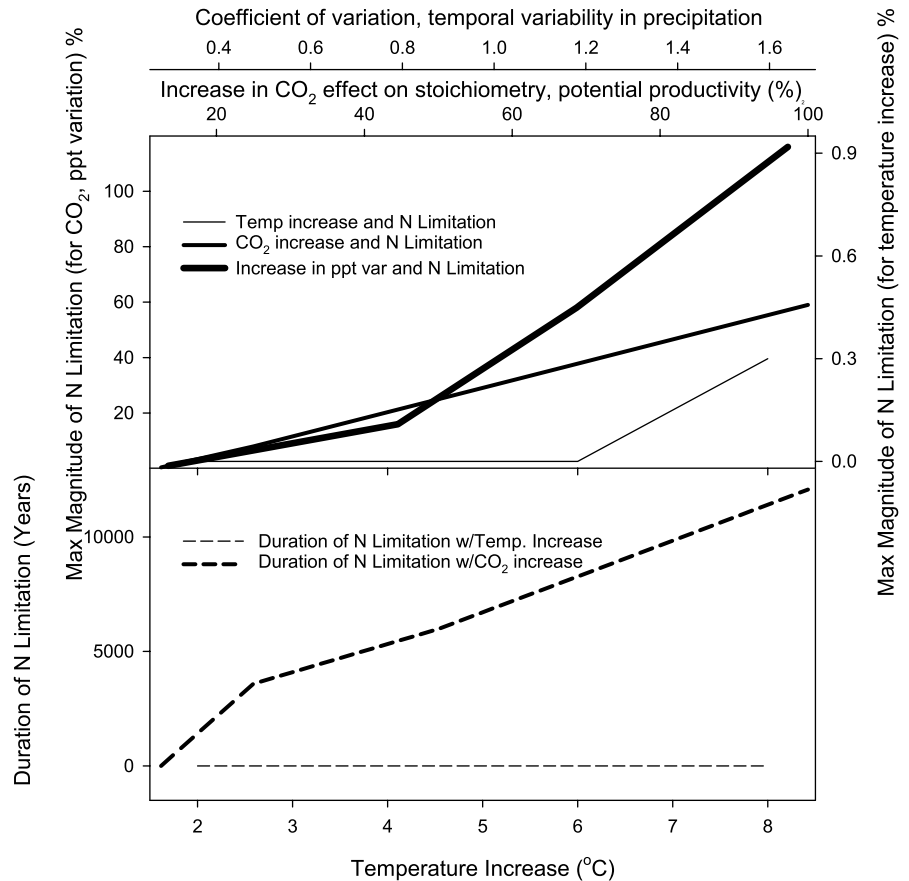
are used for NPP and N availability with increased  $\text{CO}_2$ , intermediate-thickness lines for NPP and N availability with no increased  $\text{CO}_2$ , and a thick line for NPP with N fertilization and increased  $\text{CO}_2$ . Compare NPP with and without N fertilization for the effect of increased  $\text{CO}_2$  on N limitation; compare N availability with and without increased  $\text{CO}_2$  for the effect of  $\text{CO}_2$  on N availability. There is no N limitation without increased  $\text{CO}_2$ , so the effects of N fertilization are not plotted for that case, and N availability is very high with N fertilization, so that is not plotted either

island of Hawai ‘i. Along this gradient,  $^{15}\text{N}$  in non-N-fixing plants mirrored that in soils, though with an offset of  $\sim -5$  per mil. Changing the default  $\delta^{15}\text{N}$  in precipitation from  $-5$  to  $-10$  per mil (not an unrealistically large change, for substantial sources of N from upwind ammonia volatilization in precipitation) caused an equivalent change in soil  $\delta^{15}\text{N}$  of  $-5$  per mil in the driest sites on the gradient, where atmospheric deposition was the major source of N (Fig. 7a). Even in wetter sites where BNF was a more important source of N than was atmospheric deposition, the change in  $\delta^{15}\text{N}$  of soils was close to the magnitude of the changes in  $^{15}\text{N}$  reported by Mason et al.’s (2022a, b) sources. We show the time course of changing soil  $\delta^{15}\text{N}$  in a wetter site receiving 20 cm/month of ppt, following a change from atmospheric deposition of  $^{15}\text{N}$  from  $-5$  to  $-10$  per mil after 3750 years of simulation; it decreased by  $\sim 0.45$  per mil over a century (Fig. 7b). This decrease is a large fraction of the  $\sim 1$  per mil reported by Mason et al. (2022a, b) over

150 years, even though our use of a 1-pool model for soil C and N would decrease the response to changing atmospheric deposition of  $^{15}\text{N}$ .

More generally,  $\delta^{15}\text{N}$  in ecosystems reflects both the isotope ratios in inputs of N to the ecosystem AND fractionation of N isotopes as N cycles (with enrichment of the residual N in the ecosystem caused by greater losses of N by the fractionating pathways that are more important in N-rich sites). In the short term, plants derive their N mostly from mineralization of soil N and to a small extent from atmospheric deposition, but in the longer term the  $\delta^{15}\text{N}$  of soil N (and so supply of N by mineralization) is a function of the  $^{15}\text{N}$  of N inputs. While the  $^{15}\text{N}$  in precipitation is notoriously variable, it is likely that the isotope ratios in atmospheric deposition have indeed changed in the direction suggested by Olf et al. (2022), and atmospheric deposition has likely become a larger fraction of total N inputs, making changes in  $\delta^{15}\text{N}$  difficult to interpret

**Fig. 6 A** Simulated effects of a range of CO<sub>2</sub> increases, temperature increases, and temporal variability in precipitation on the magnitude of N limitation. CO<sub>2</sub> increases are reported as a percentage increase in potential productivity and the C-richness of plant stoichiometry; temporal variation in precipitation is reported in terms of its Coefficient of Variation (CV, std. variation/mean). **B.** Simulated effects of a range of CO<sub>2</sub> increases and temperature increases on how long N limitation persists (how many years N fertilized model runs differ by at least 0.5% from unfertilized model runs). The effects of temporal variation in precipitation are not reported here because this is an equilibrium change that is never reversed by atmospheric deposition of N in remote areas



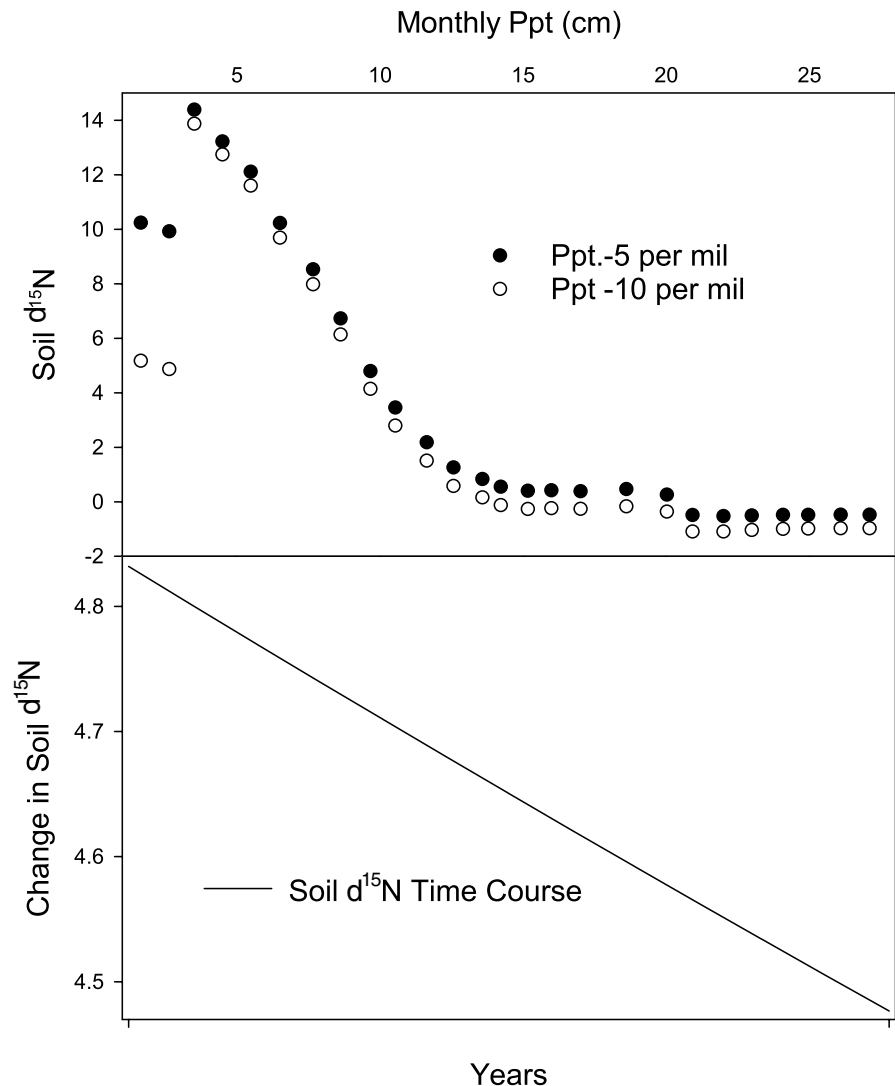
as reflecting simply changes in N availability. It is important to note that changes in the <sup>15</sup>N of N inputs due to ammonia volatilization associated with agriculture or fossil fuel combustion occur over a subset of Earth's surface while increased temperatures and atmospheric CO<sub>2</sub> affect the entire planet.

The model on which we based our analysis is limited by its assumptions, as all models are. In particular, the model was calibrated for a particular rainfall gradient in Hawai 'i. While we believe the model to be general except for the influences of volcanically-derived clays, those clays could be important in shaping δ<sup>15</sup>N, as described above. Also, net mineralization is modeled here; plants do not compete with microbes for available soil N in the model. That is appropriate for our focus on N losses, in that otherwise available forms of N will not be lost from ecosystems where plants and their mycorrhizae do compete with decomposers, but it is a constraint on the generalizability of the model.

## Conclusions

Results of our model-based analysis show that there are plausible mechanisms by which components of anthropogenic global change could cause reduced N availability and induce N limitation. Some of these mechanisms, notably increased precipitation variability caused by climate change and ecosystem-level disturbance, could drive reduced N availability and the development of N limitation at equilibrium. Other changes especially including increasing atmospheric CO<sub>2</sub> could cause non-equilibrium (but for CO<sub>2</sub> large and long-lasting) declines in N availability and the development of N limitation—if there are constraints to the responsiveness of BNF to N deficiency. Still other changes, such as decreasing acid rain or decreases on atmospheric pollutants such as ozone that now decrease plant production and demand for N could also cause increased limitation if they occur rapidly enough. Anthropogenic global change means that Earth is out of equilibrium, if it was ever in it,

**Fig. 7** **A** Simulated effects of changing the  $^{15}\text{N}$  abundance in atmospheric deposition from -5 per mil to -10 per mil, calculated for  $\delta^{15}\text{N}$  in ecosystems across a climate gradient in Hawaii 'i using the program *nitrft-graddeep* with deep soils included and BNF on.  $\delta^{15}\text{N}$  in soils for atmospheric deposition of -5 per mil is shown with solid symbols and that with atmospheric deposition of -10 per mil with hollow symbols. The two driest sites receive most of their N from atmospheric deposition, while the wetter sites have a greater input from BNF. **B** Time course of change in soil  $\delta^{15}\text{N}$  over 100 years (1200 months) in a site receiving 20 cm/month precipitation, using the program *tcnewprodno-fixcr* with BNF off



broadening the conditions under which N limitation can be more than marginal and/or ephemeral.

These results do not suggest that excessive N enrichment associated with high rates of atmospheric deposition and/or urban and agricultural land use are not important environmental problems in many areas. Still, it is important to recognize that these problems occur over relatively small areas, while other components of anthropogenic global change such as increased atmospheric  $\text{CO}_2$  affect the entire planet. Reductions in N availability over the vast areas of Earth that are little-affected by N enrichment could have important effects on net primary production, carbon sequestration, trophic

dynamics and other ecosystem functions and services.

**Acknowledgements** We thank Rachel Mason, Andrew Elmore, Han Olf, Rien Aerts, and David Wardle for comments on earlier drafts of this manuscript.

**Author contributions** PV wrote and ran the model used for this work, and wrote the first draft of the manuscript. Xiaoyu Cen and Peter Groffman revised the manuscript and approved its submission.

**Funding** Research supported by NSF Grant ETBC 1020791 to Peter Vitousek.

**Data availability** The model used for this analysis is provided as supplementary material. If results of model runs are

desired by readers, they will be provided by the corresponding author upon reasonable request.

## Declarations

**Conflict of interest** The authors declare no competing financial or non-financial interests or conflicts.

**Open Access** This article is licensed under a Creative Commons Attribution 4.0 International License, which permits use, sharing, adaptation, distribution and reproduction in any medium or format, as long as you give appropriate credit to the original author(s) and the source, provide a link to the Creative Commons licence, and indicate if changes were made. The images or other third party material in this article are included in the article's Creative Commons licence, unless indicated otherwise in a credit line to the material. If material is not included in the article's Creative Commons licence and your intended use is not permitted by statutory regulation or exceeds the permitted use, you will need to obtain permission directly from the copyright holder. To view a copy of this licence, visit <http://creativecommons.org/licenses/by/4.0/>.

## References

- Bennett EM, Carpenter SR, Caraco NF (2001) Human impact on erodible phosphorus and eutrophication: a global perspective. *Bioscience* 51:227–234
- Burnett MW, Bobbett AE, Brendel CB, Marshall K, von Sperber C, Paulus EL, Vitousek PM (2022) Biological nitrogen fixation across pedogenic thresholds, Hawai'i Island, USA. *Oecologia* 198:229–242
- Chadwick OA, Chorover J (2001) The chemistry of pedogenic thresholds. *Geoderma* 100:321–353
- Davidson EA, de Carvalho CJR, Vieira ICG, Figueiredo RO, Moutinho P, Ishida FY, dos Santos MTP, Guerrero JB, Kalif K, a& Sabá RT. (2004) Nutrient limitation of biomass growth in a tropical secondary forest: early results of a nitrogen and phosphorus amendment experiment. *Ecol Appl* 14:S150–S163
- Falkowski PG, Fenchel T, DeLong EF (2008) The microbial engines that drive Earth's biogeochemical cycles. *Science* 320:1035–1039
- Firestone MK, Davidson EA (1989) Microbiological basis of NO and N<sub>2</sub>O production and consumption in soil. In: Andreae MO, Schimel DS (eds) Exchange of trace gases between terrestrial ecosystems and the atmosphere. Wiley, Chichester, pp 7–21
- Fowler D, Coyle M, Skiba U, Sutton MA, Cape JN, Reis S, Sheppard LJ, Jenkins A, Grizzetti B, Galloway JN, Vitousek P, Leach A, Bouwman AF, Butterbach-Bahl K, Dentener F, Stevenson D, Amann M, Voss M (2013) The global nitrogen cycle in the twenty-first century. *Philos Trans R Soc B* 368(1621):20130164. <https://doi.org/10.1098/rstb.2013.0164>
- Galloway JN, Townsend AR, Erisman JW, Bekunda M, Cai Z, Freney JR, Seitzinger SP, Sutton MA (2008) Transformation of the nitrogen cycle: recent trends questions, and potential solutions. *Science* 320:889–892
- Giambelluca TW, Chen Q, Frazier AG, Price JP, Chen Y-L, Chu P-S, Eischeid JK, Delparte DM (2013) Online Rainfall Atlas of Hawai'i. *Bull Amer Meteor Soc* 94:313–316
- Granger J, Wankel SD (2016) Isotope overprinting of nitrification on denitrification as a ubiquitous and unifying feature of environmental nitrogen cycling. *PNAS*. <https://doi.org/10.1073/pnas.1601383113>
- Groffman PM, Driscoll CT, Duran J, Campbell JL, Christenson LM, Fahey TJ, Fisk MC, Fuss C, Likens GE, Lovett G, Rustad L, Templer PH (2018) Nitrogen oligotrophication in northern hardwood forests. *Biogeochemistry* 141:523–539. <https://doi.org/10.1007/s10533-018-0445-y>
- Gu B, Ju X, Chang J, Ge Y, Vitousek PM (2015) Integrated reactive nitrogen budgets and future trends in China. *PNAS* 112:8792–8797
- Hedin LO, Armesto JJ, Johnson AH (1995) Patterns of nutrient loss from unpolluted, old-growth temperate forests: evaluation of biogeochemical theory. *Ecology* 76:493–509
- Herridge DF, Peoples MB, Boddey RM (2008) Global inputs of biological nitrogen fixation in agricultural systems. *Plant Soil* 311:1–18
- Houlton BZ, Sigman DM, Hedin LO (2006) Isotopic evidence for large gaseous losses from tropical rainforests. *PNAS* 103:8745–8750
- Hungate BA, Dukes JS, Shaw MR, Luo Y, Field CB (2003) Nitrogen and climate change. *Science* 302:1512–1513
- Kramer MG, Sanderman J, Chadwick OA, Chorover J, Vitousek P (2012) Long-term carbon storage through retention of dissolved aromatic acids by reactive particles in soil. *Glob Change Biol* 18:2594–2605
- Kharin VV, Zwiers FW, Zhang X-B, Hegerl GC (2007) Changes in temperature and precipitation extremes in the IPCC ensemble of global coupled model simulations. *Climate* 20:1419–1444
- Liu X, Zhang Y, Han W, Tang A, Shen J, Cui Z, Vitousek P, Erisman JW, Goulding K, Christie P (2013) Enhanced nitrogen deposition over China. *Nature* 494(7438):459–462. <https://doi.org/10.1038/nature11917>
- Mariotti A, Germon JC, Hubert P, Kaiser P, Letolle R, Tardieu A, Tardieu P (1981) Experimental determination of nitrogen kinetic isotope fractionation: some principles; illustration for the denitrification and nitrification processes. *Plant Soil* 62:413–430
- Mason RE, Craine JM, Lany NK, Jonard M, Ollinger SV, Groffman PM, Fulweiler RW, Angerer J, Read QD, Reich PB, Templer PH, Elmore AJ (2022a) Evidence, causes, and consequences of declining nitrogen availability in terrestrial ecosystems. *Science* 376:261. <https://doi.org/10.1126/science.abh3767>
- Mason RE, Craine JM, Lany NK, Jonard M, Ollinger SV, Groffman PM, Fulweiler RW, Angerer J, Read QD, Reich PB, Templer PH, Elmore AJ (2022b) Response. *Science* 376:1170
- McKey D (1994) Legumes and nitrogen: the evolutionary ecology of a nitrogen-demanding lifestyle. In: Sprent JJ, McKey D (eds) *Advances in legume systematics* 5: the

- nitrogen factor. Royal Botanical Gardens, London, pp 211–226
- Menge DNL (2011) Conditions under which nitrogen can limit steady state net primary production in a general class of ecosystem models. *Ecosystems* 14:519–532
- Menge DNL, Levin SA, Hedin LO (2008) Evolutionary tradeoffs can select against nitrogen fixation and thereby maintain nitrogen limitation. *Proc Nat Acad Sci USA* 105:1573–1578
- Menge DNL, Levin SA, Hedin LO (2009) Facultative versus obligate nitrogen fixation strategies and their ecosystem consequences. *Am Nat* 174:465–477
- Nixon SW (1995) Coastal marine eutrophication: A definition, social causes, and future concerns. *Ophelia* 41:199–219. <https://doi.org/10.1080/00785236.1995.10422044>
- Olf H, Aerts R, Bobbink R, Cornelissen JHC, Erisman JW, Galloway JN, Stevens CJ, Sutton MA, de Vries FT, Wamelink GWW, Wardle DA (2022) Explanations for nitrogen decline. *Science* 376:1169–1170
- Pendergrass AG, Knuti R, Lehner F, Deser C, Sander-son BM (2017) Precipitation variability increases in a warmer climate. *Sci Rep* 1:10. <https://doi.org/10.1038/s41598-017-17966-y>
- Peng L, Limin T, Shutan M, Xi W, Ruhai W, Yonghui T, Wang L, Ti C, Yan X (2022)  $^{15}\text{N}$  natural abundance characteristics of ammonia volatilization from soils applied by different types of fertilizer. *Atmosphere* 13:1566. <https://doi.org/10.3390/atmos13101566>
- Peñuelas J, Martínez MF, Vallicrosa H, Maspons J, Zuccanini P, Carnicer J, Sanders TGM, Kruger I, Obersteiner M, Janssens IA, Ciais P, Sardans J (2020) Increasing atmospheric  $\text{CO}_2$  concentrations correlate with declining nutritional status of European forests. *Commun Biol* 3:125
- Perakis SS, Hedin LO (2001) Fluxes and fate of inorganic nitrogen in an unpolluted old-growth rainforest in southern Chile. *Ecology* 82:2245–2260
- Perakis SS, Hedin LO (2002) Nitrogen loss from unpolluted South American forests mainly via dissolved organic compounds. *Nature* 415:416–419
- Rastetter EB (2017) Modeling for understanding v. modeling for numbers. *Ecosystems* 20:215–221
- Robinson D (2001)  $\delta^{15}\text{N}$  as an integrator of the nitrogen cycle. *Trends Ecol Evol* 16:153–162. [https://doi.org/10.1016/S0169-5347\(00\)02098-X](https://doi.org/10.1016/S0169-5347(00)02098-X)
- Stocker BD, Prentice IC, Cornell SE, Davies-Barnard T, Finzi AC, Franklin O, Janssens I, Larmola T, Manzoni S, Nasholm T, Raven JA, Rebel KT, Reed S, Vicca S, Wiltshire A, Zaehle S (2016) Terrestrial nitrogen cycling in Earth system models revisited. *New Phytol* 210:1165–1168. <https://doi.org/10.1111/nph.13997>
- Ti C, Ma S, Peng L, Tao L, Wang X, Dong W, Wang I, Yan X (2021) Changes of  $\delta^{15}\text{N}$  values during the volatilization process after applying urea on soil. *Environ Pollut* 270:116204. <https://doi.org/10.1016/j.envpol.2020.116204>
- Vitousek PM (2004) Nutrient cycling and limitation: Hawaii as a model system. Princeton University Press, Princeton, NJ
- Vitousek PM, Field CB (1999) Ecosystem constraints to symbiotic nitrogen fixers: a simple model and its implications. *Biogeochemistry* 46:179–202
- Vitousek PM, Shearer G, Kohl DH (1989) Foliar  $^{15}\text{N}$  natural abundance in Hawaiian rainforest: patterns and possible mechanisms. *Oecologia* 78:383–388
- Vitousek PM, Menge DNL, Reed SC, Cleveland CC (2013) Biological nitrogen fixation: rates, patterns and ecological controls in terrestrial ecosystems. *Philos Trans R Soc B* 368:20130119
- Vitousek PM, Bateman JB, Chadwick OA (2021) A “toy” model of biogeochemical dynamics on climate gradients. *Biogeochemistry* 154:183–210. <https://doi.org/10.1007/s10533-020-00734-y>
- Vitousek PM, Treseder KK, Howarth RW, Menge DNL (2022) A “toy model” analysis of causes of Nitrogen limitation in terrestrial ecosystems. *Biogeochemistry* 160:381–394. <https://doi.org/10.1007/s10533-022-00959-z>
- von Sperber C, Chadwick OA, Casciotti KL, Peay KG, Francis CA, Kim AE, Vitousek PM (2017) Controls of nitrogen cycling along a well-characterized climate gradient on Kohala Volcano, Hawaii. *Ecology*. <https://doi.org/10.1002/ecy.1751>
- Wang R, Balkanski Y, Boucher O, Ciais P, Peñuelas J, Tao S (2015) Significant contribution of combustion-related emissions to the atmospheric phosphorus budget. *Nat Geosci* 8(1):48–54. <https://doi.org/10.1038/ngeo2324>

**Publisher's Note** Springer Nature remains neutral with regard to jurisdictional claims in published maps and institutional affiliations.